Heliyon 9 (2023) e21846

Contents lists available at ScienceDirect

Heliyon

journal homepage: www.cell.com/heliyon

Korean red ginseng formula attenuates non-alcoholic fatty liver disease in oleic acid-induced HepG2 cells and high-fat diet-induced rats

Min Zheng [a,b,1], Yang Li [a,b,1], Zhiying Dong [a,b], Yibo Zhang [a,b], Zhichao Xi [a,b], Man Yuan [a,b,**], Hongxi Xu [c,*]

[a] School of Pharmacy, Shanghai University of Traditional Chinese Medicine, Shanghai, 201203, China
[b] Engineering Research Center of Shanghai Colleges for TCM New Drug Discovery, Shanghai, 201203, China
[c] Shuguang Hospital, Shanghai University of Traditional Chinese Medicine, Shanghai, 201203, China

ARTICLE INFO

Keywords:
Non-alcoholic fatty liver disease
Triglyceride
Cholesterol
Korean red ginseng
Hyperlipidemia
Steatosis

ABSTRACT

Objective: Non-alcoholic fatty liver disease (NAFLD) is the leading chronic liver disease. We have developed a Korean Red Ginseng Formula (KRGF) containing extracts of Korean Red Ginseng (KRG), Crataegus Fructus, and Cassiae Semen. In this study, our aims were to investigate the therapeutic potential and underpinning mechanisms of KRGF in NAFLD complicated by hyperlipidemia.

Methods: In the *in vitro* assays, HepG2 cells were treated with KRGF for 24 h in the presence or absence of oleic acid (OA). To assess the *in vivo* protective effect of KRGF against NAFLD, rats fed a high-fat diet (HFD) were given intragastric administration for 30 days.

Results: KRGF exerted protective effects against NAFLD by reducing lipid accumulation and steatosis in OA-stimulated HepG2 cells and HFD-fed rats. In HFD-fed rats, KRGF effectively decreased triglyceride levels in both blood and liver tissue and modulated the expression of key regulators of lipogenesis and fatty acid oxidation. KRGF downregulated the expression of lipogenesis factors, namely C/EBPα, FAS, SREBP-1c, and PPARγ, while upregulating the expression of PPARα and CPT-1, thus promoting fatty acid oxidation. Additionally, KRGF intensified the phosphorylation of AMPK and ACC, which are two enzymes that suppress fatty acid synthesis and promote fatty acid oxidation. KRGF effectively decreased total cholesterol (TC) levels in both blood and liver tissue, and it modulated the expression of major enzymes related to TC metabolism, namely apoB, ACAT2, CYP7A1, and HMGCR.

Conclusion: In conclusion, KRGF mitigated NAFLD complicated by hyperlipidemia by modulating triglyceride and cholesterol metabolism, suggesting its potential for future development in the treatment of NAFLD.

* Corresponding author. Shuguang Hospital, Shanghai University of Traditional Chinese Medicine, Shanghai, 201203, China.
** Corresponding author. School of Pharmacy, Shanghai University of Traditional Chinese Medicine, Shanghai, 201203, China.
E-mail addresses: peggyyuan1990@163.com (M. Yuan), xuhongxi88@gmail.com (H. Xu).
[1] These authors have contributed equally to this work.

https://doi.org/10.1016/j.heliyon.2023.e21846
Received 18 July 2023; Received in revised form 29 October 2023; Accepted 30 October 2023
Available online 4 November 2023

1. Introduction

Non-alcoholic fatty liver disease (NAFLD) is the leading chronic liver disease worldwide with a prevalence of 32.4 % [1–3]. NAFLD is resulted from abnormal metabolism rather than alcohol or drug consumption, and it is characterized by the deposition of more than 5 % fat in liver cells [4]. The pathogenesis of NAFLD is complex, and remains unclear. The "multiple parallel hits" hypothesis, which involves insulin resistance, lipotoxicity, inflammation, genetic polymorphism and epigenetics, adipokines and hepatokines, bile acid, and gut microbiota, has replaced the "two hits" hypothesis to explain NAFLD's pathogenesis [5,6]. NAFLD includes simple steatosis (NAFL), steatohepatitis (NASH), fibrosis, and cirrhosis, all of which signify a risk of developing hepatocellular carcinoma. Effective preventive and therapeutic pharmacotherapies are lacking [7].

Numerous herbal formulations and medicinal plants hold therapeutic potential for the treatment of NAFLD due to their diverse effects and minimal side effects. The potential therapeutic effects of Korean Red Ginseng (KRG, *Panax ginseng* C.A. Meyer) include addressing dyslipidemia and NAFLD [8]. In KRG-treated rats, lipid profiles and steatohepatitis were improved compared to those in the NAFLD group [9]. The combination of KRG and other botanical therapeutic ingredients, including Cordyceps militaris [10], *Glycyrrhiza glabra* L. extract [11] and Radix Bupleuri [12], has shown anti-obesity, NAFLD protective, lipid-regulating, and anti-inflammatory properties. Additionally, Crataegus Fructus and Cassiae Semen have been investigated as potential treatment options for NAFLD and metabolic syndrome [13,14]. Crataegus Fructus extract significantly decreased liver tissue fat and total cholesterol levels, and reduced liver weight in rodents with diet-induced steatosis [13,15]. Cassiae Semen and its components protect against NAFLD by alleviating hepatic steatosis, intestinal barrier damage, lipid metabolism disorders, and inflammation [14,16,17].

Mixtures of two or more natural products in varying proportions have more pronounced effects than single natural products [18], possibly due to synergies between them [19]. Based on an extensive literature review, several Chinese medicines with hypolipidemic effects were selected. These included Crataegus Fructus, Pueraria Lobatae Radix [20], Atractylodis Macrocephalae Rhizoma [21], Salviae Miltiorrhiza Radix et Rhizoma [22], Cassiae Semen, Glycyrrhizae Radix et Rhizoma [23], and Red Yeast Rice [24]. Ginkgo Leaves extract, Soybean Lecithin, and Fish Oil had been selected as controls. By comparing the inhibitory effects on lipid accumulation, Crataegus Fructus and Cassiae Semen were preliminarily chosen to create a formula with Korean Red Ginseng. The optimal proportion of extracts was ultimately determined and named as Korean Red Ginseng Formula (KRGF). This study explored the therapeutic actions and mechanisms of KRGF in treating NAFLD. Steatosis was induced in HepG2 cells *in vitro* by exposing them to oleic acid (OA), and NAFLD was induced in rats *in vivo* by providing them with high-fat diet (HFD).

2. Materials and methods

2.1. Materials

Crataegus Fructus, Pueraria Lobatae Radix, Atractylodis Macrocephalae Rhizoma, Salviae Miltiorrhiza Radix et Rhizoma, Cassiae Semen, Glycyrrhizae Radix et Rhizoma, Red Yeast Rice, and Ginkgo Leaves extracts were procured from Shaanxi Jiahe Phytochem Co., Ltd. Soybean Lecithin and Fish Oil were sourced from Shanghai Shanghai Biotechnology Co., Ltd. Red Ginseng extract (50 % yield) was purchased from the Korean Ginseng Corporation.

As per the information provided by Shaanxi Jiahe Phytochem Co., Ltd, the raw material of Crataegus Fructus (*Crataegus pinnatifida* Bge.) was subjected to double extraction with 60 % ethanol for 1.5 h each time. The resultant extract was concentrated and vacuum belt-dried, producing an extract powder with a 20 % yield. Similarly, the raw material of Cassiae Semen (*Cassia tora* Linn) was extracted three times with 60 % ethanol for 1.5 h each time. The resulting extraction solution was concentrated and spray-dried, yielding an extract powder with a 7 % yield.

The composition of KRGF consists of 1.5 g Red Ginseng, 1.8 g Crataegus Fructus, and 0.6 g Cassiae Semen extracts in a specific weight proportion. The KRGF Tablet (KRGT, 4 g per tablet) was formulated with 1.5 g Red Ginseng extract, 1.8 g Crataegus Fructus extract, 0.6 g Cassiae Semen extract, and 0.1 g of pharmaceutical excipient, all provided by the Cosmax Bio Company.

2.2. Cell culture

HepG2 cells were obtained from the American Type Culture Collection (Manassas, VA, USA) and cultured in Dulbecco's Modified Eagle medium (DMEM) supplemented with 10 % fetal bovine serum and 1 % antibiotic-antimycotic (Gibco, Grand Island, NY) at 37 °C in a humidified atmosphere with 5 % CO_2 [25]. HepG2 cells grown to 80 % confluence and subsequently treated with serum-free DMEM containing 1 % bovine serum albumin (BSA) or oleic acid (OA) for 24 h or 48 h.

2.3. Cell viability analysis

The MTT assay (3-(4,5-dimethylthiazol-2-yl)-2,5-diphenyl tetrazolium bromide; Sigma Aldrich, MO, USA) was conducted to evaluate the cytotoxic effects of tested samples, including Crataegus Fructus extract, Pueraria Lobatae Radix extract, Atractylodis Macrocephalae Rhizoma extract, Salviae Miltiorrhiza Radix et Rhizoma extract, Cassiae Semen extract, Glycyrrhizae Radix et Rhizoma extract, Red Yeast Rice extract, Ginkgo Leaves extract, Soybean Lecithin, and Fish Oil. The assay aimed to determine optimal concentrations for treating HepG2 cells. HepG2 cells were seeded in 96-well plates and cultured until reaching 80 % confluence. Subsequently, the cells were exposed to the tested samples at various concentrations (1–100 μg/mL) for 48 h. Following this exposure, the MTT assay was performed as previously described [26]. The absorbance at 490 nm was measured using a microplate reader

(PerkinElmer, USA). Cell viability (%) was calculated as follows: (A490 nm $_{(\text{tested sample})}$/A490 nm $_{(\text{control})}$) × 100.

To establish the appropriate concentration of OA for inducing steatosis using the CCK-8 assay, different concentrations of OA (0.2–3 mM) and KRGF (62.5–2000 μg/mL) were individually applied to HepG2 cells and incubated for 24 h. Upon selecting 0.8 mM as the suitable concentration of inducing steatosis *in vitro*, HepG2 cells were exposed to 0.8 mM OA and KRGF (62.5–2000 μg/mL) for 24 h. The CCK-8 assay was performed as previously described method [25], and absorbance at 450 nm was measured using a microplate reader. Cell viability (%) was calculated as (A450 nm $_{(\text{treatment})}$/A450 nm $_{(\text{control})}$) × 100.

2.4. Staining with Oil Red O

Cells were fixed in 4 % paraformaldehyde in PBS for 15 min, stained with Oil Red O solution at room temperature for 10 min, and then washed thrice with PBS [27]. Cellular steatosis levels were assesed by examining red-stained cells using an inverted fluorescence microscope (Olympus, Tokyo, Japan) and taking photographs.

2.5. Quantification of intracellular levels of TG and TC

When HepG2 cells reached 80 % confluence, they were treated with 0.8 mM OA, with or without KRGF (0, 62.5, 125, and 250 μg/mL) for 24 h. KRGF was diluted in serum-free DMEM containing 1 % BSA. Control cells were exposed to 1 % BSA only. Quantification of triglyceride (TG) and total cholesterol (TC) contents in HepG2 cells was performed following the manufacturer's instructions (TG and TC Content Assay Kits; Boxbio Science & Technology Co., Ltd., Beijing, China).

2.6. Animals, diets, and treatments

We obtained 6-week-old SPF male Wistar rats from the Experimental Animal Center of Shanghai University of Traditional Chinese Medicine and ensured animal care adhered to institutional guidelines. These rats were housed in a SPF-level facility with a temperature of 22 ± 2 °C, humidity ranging from 50 % to 70 %, and a 12-h light/dark cycle. Approval for this animal experiment was granted by the Animal Experiment Ethics Committee of Shanghai University of Traditional Chinese Medicine (No. PZSHUTCM201106015; No. PZSHUTCM210709002).

Initially, we examined the therapeutic effects of KRGF and its underlying mechanisms in a NAFLD rat model. The rats were allowed to acclimate to their new surroundings for a week before randomly assigned to the normal control and NAFLD model groups. During the modeling period, the rats were provided with either a normal diet or HFD with unrestricted access to food and water for 4 weeks. Subsequently, the rats were randomized into five groups, each consisting of eight rats: normal control (NC), HFD-induced control (HF), HFD with low-dose KRGF (LD, 325 mg/kg/day), HFD with high-dose KRGF (HD, 650 mg/kg/day), and HFD with fenofibrate (PC, 25 mg/kg/day). The KRGF group received the corresponding KRGF dose, whereas the PC group was administered fenofibrate by gavage for 30 days, and the NC and HF groups received intragastric water only. Food consumption and body weight were recorded on alternate days.

Another experiment was conducted to evaluate the lipid-lowering effects of KFGT in the NAFLD rat model. The rats were randomly divided into six groups, each consisting of nine rats, after being fed either a normal diet or HFD for 3 weeks. The groups were as follows: normal control group (NC), HFD-induced control group (HF), HFD with 2.5 times the dose of KRGT group (2.5 × KRGT, 166.7 mg/kg/day), HFD with 5 times the dose of KRGT group (5 × KRGT, 333.3 mg/kg/day), HFD with 10 times the dose of KRGT group (10 × KRGT, 666.7 mg/kg/day), and HFD with 20 times the dose of KRGT group (20 × KRGT, 1333.3 mg/kg/day). The treatment groups were administered with the corresponding dose of KRGT by gavage for 30 days, while the NC and HF groups received only drinking water. To verify the lipid-lowering effect of KRGT, the rats' food consumption and body weight were measured on alternate days.

2.7. Sampling of blood and tissue

To obtain serum samples, blood was drawn from the treated rats through the post-orbital venous plexus and then centrifuged for 15 min at 3000 rpm and 4 °C. The rats were anesthetized and euthanized, and their liver tissues were harvested and weighed. A portion of the liver tissue samples was fixed in 4 % paraformaldehyde for pathological examination, while the remaining sections were preserved in liquid nitrogen.

2.8. Analysis of serum lipids

Serum triglyceride (TG), total cholesterol (TC), high-density lipoprotein cholesterol (HDL-C), and low-density lipoprotein cholesterol (LDL-C) levels were determined using an automatic biochemical analyser in accordance with the manufacturer's protocol (TBA-40FR, Toshiba Medical Instruments, Tochigi-ken, Japan).

2.9. Histological analysis of liver tissue

Liver tissue was fixed in 4 % paraformaldehyde, embedded in paraffin, sectioned, and stained with hematoxylin and eosin (H&E), and then observed and photographed using an optical microscope (Olympus, Tokyo, Japan).

2.10. Measurement of hepatic TG and TC

To measure hepatic TG, 100 mg of liver tissue samples were retrieved, homogenized in 1 mL of n-heptane/isopropanol (1:1 by volume) solution, and then centrifuged at 8000 rcf for 10 min at 4 °C. The TG content in the supernatant was measured following the manufacturer's instruction (Boxbio Science & Technology Co., Ltd., Beijing, China). For TC measurement, 100 mg of the resected liver tissue samples were homogenized in 1 mL of isopropanol and centrifuged at 10000 rcf for 10 min at 4 °C. The TC content in the supernatant was determined following the test kit's instruction (Boxbio Science & Technology Co., Ltd., Beijing, China).

2.11. Quantitative real-time PCR (qRT-PCR)

RNAiso plus reagent (TaKaRa Biotechnology, Otsu, Shiga, Japan) was used to isolate total RNA from the liver tissue. Subsequently, a reverse transcription kit (PrimeScript™ RT Reagent Kit; TaKaRa Biotechnology, Otsu, Shiga, Japan) was utilized for reverse transcription into cDNA. Quantitative real-time polymerase chain reaction (qRT-PCR) was conducted using a StepOne Plus Real-Time PCR system (Applied Biosystems, Life Technologies) following a previously described protocol [28]. SYBR® Green Realtime PCR Master Mix (TOYOBO Life Science, Osaka, Japan) was used for the reactions. The primer sequences used in these experiments are listed in Table 1. GAPDH was applied as an internal reference for normalization, and the expression of the target genes was calculated using the $2^{-\Delta\Delta CT}$ method.

2.12. Western blotting

To obtain protein samples, cells and liver tissue samples were lysed using a mixture containing protease inhibitors, phosphatase inhibitors, PMSF, and pre-cooled RIPA lysis buffer (WellBio Technology Co., Ltd, Shanghai, China). Protein quantification, electrophoresis, and Western blot were performed following established protocols [28]. Primary antibodies against CCAAT/enhancer-binding protein alpha (C/EBPα; sc-166258), peroxisome proliferator-activated receptor alpha (PPARα; sc-398394), sterol regulatory element-binding protein-1c (SREBP-1c; sc-13551), and AMP-activated protein kinase (AMPK; sc-74461) were acquired from Santa Cruz Biotechnology (Dallas, CA, USA). Primary antibodies against GAPDH (60004-1-Ig), carnitine palmitoyltransferase-1 (CPT-1, 15184-1-AP), and PPARγ (16643-1-AP) were purchased from Proteintech (Wuhan, Hubei, China). Primary antibodies against phospho-AMPK (*p*-AMPK, #2535), fatty acid synthase (FAS, #3180), acetyl-CoA carboxylase (ACC, #3676), and phospho-ACC (*p*-ACC, #11818) were supplied by Cell Signaling Technology (Danvers, Massachusetts, USA). Protein expression was detected using an enhanced chemiluminescence kit, and visualized with an ImageQuant LAS 4000 Mini instrument (GE Healthcare Bio-Sciences AB, Sweden). Protein band gray values were quantified using ImageJ software.

2.13. Statistical analysis

The experiments were performed in triplicate, and the data were presented as the mean ± SD. The data were analyzed using GraphPad Prism 8.0, employing one-way analysis of variance (ANOVA) and Student's *t*-test. The statistical p-value was set less than 0.05.

Table 1
Primer sequence used for quantitative real-time PCR.

	Gene	Forward (5′-3′)	Reverse (5′-3′)
Rat liver	ACAT2	TACTGATGGGACTGGAACG	CTTGCTTTATGGCTGGAAT
	HMGCR	CAACCTCTACATCCGTCTCC	AGTGCTTTCTCCGTACCCT
	apoB	GACCTGGGTGAACCTAACT	AGACTGTATCCTGGAACAAAA
	CYP7A1	GGGTCACGGAAGGGATGTA	GTGCCGGAAAGACTTGGTC
	SREBP-1c	CTGGGCTCCTCTCTGGAA	GGCACTGGCTCCTCTTTG
	ACC	GGTGGTTCTTGGGTTGTGA	TTTCTACTGTCCCTTCTGGTT
	FAS	TGATGATTCAGGGAACGGGTAT	GGGAATGTCACGCCTTGCT
	PPARα	AGAATCCACGAAGCCTACC	TCTTCTCAGCCATGCACA
	C/EBPα	GTGAGTTCGTGGAGAAGGG	TACACACAAGGCGGATGG
	CPT-1	CAGGGATACAGAGAGGAG	TTGAAGACAACAAAGGTG
	PPARγ	ACCCTTTACCACGGTTGA	CAGGCTCTACTTTGATCGC
	GAPDH	TCTCTGCTCCTCCCTGTTC	ACACCGACCTTCACCATCT

ACAT2, acetyl-CoA acyltransferase 2; HMGCR, 3-hydroxy-3-methylglutaryl-CoA reductase; apoB, apolipoprotein B; CYP7A1, cholesterol 7 alpha-hydroxylase; SREBP-1c, sterol regulatory element binding protein-1c; ACC, acetyl-CoA carboxylase; FAS, fatty acid synthase; PPARα, peroxisome proliferator-activated receptor alpha; C/EBPα, CCAAT/enhancer-binding protein alpha; CPT-1, carnitine palmitoyltransferase-1; PPARγ, peroxisome proliferator-activated receptor gamma; GAPDH, glyceraldehyde-3-phosphate dehydrogenase.

3. Results

3.1. Examination of Korean Red Ginseng Formula (KRGF)

We conducted a MTT assay to evaluate the cytotoxicity of the tested samples at various concentrations (1–100 μg/mL) in HepG2 cells. In this experiment, when the cell viability is above 80 %, the sample was considered to be non-cytotoxic and can be used for subsequent screening experiments. Fig. 1Ã J display the highest concentrations of 10 tested samples that do not induce cytotoxicity, as

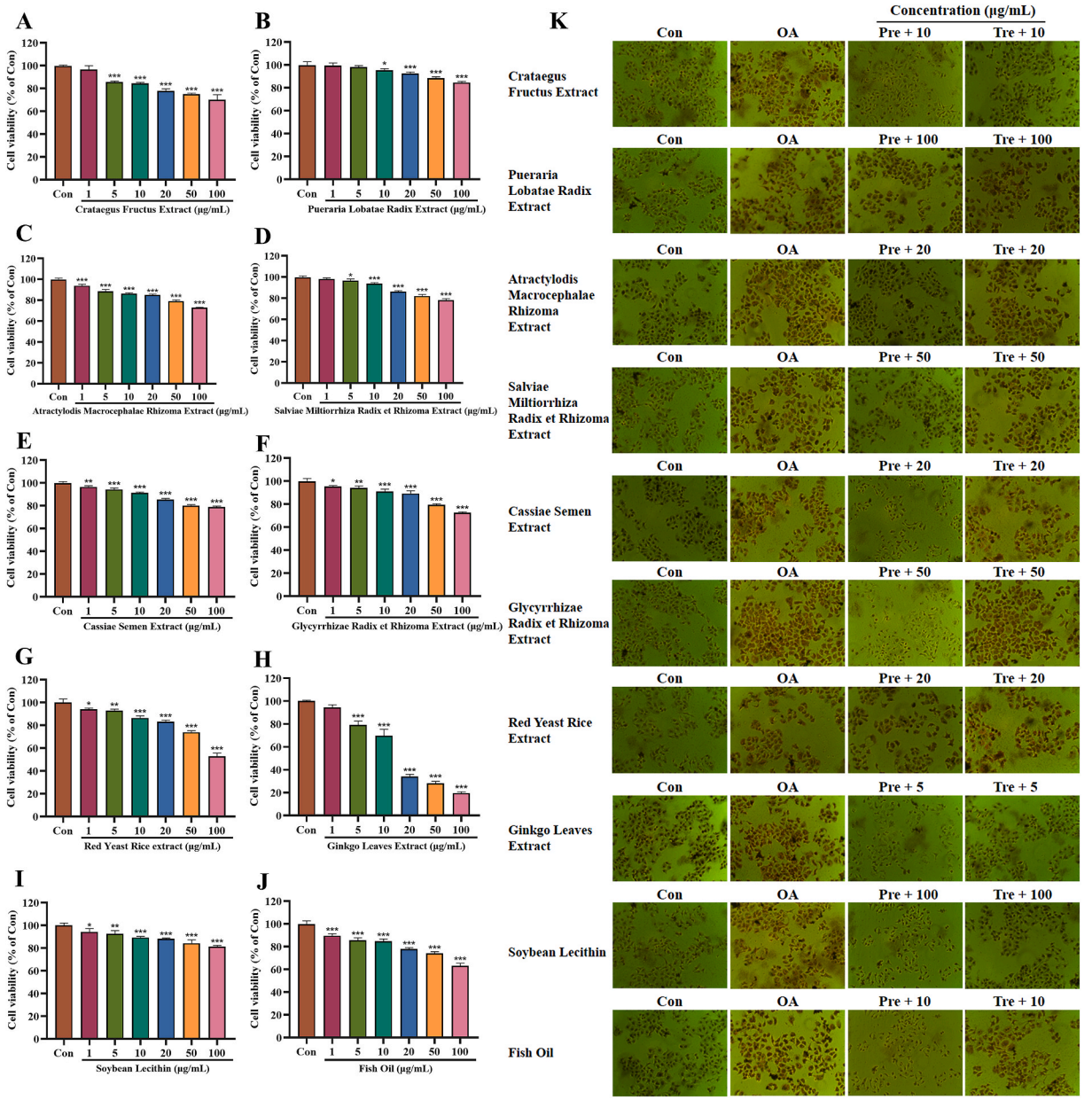

Fig. 1. Cytotoxicity and lipid accumulation in OA-induced HepG2 cells. Cell viability was measured after exposing HepG2 cells to various concentrations (0–100 μg/mL) of 10 different samples for 48 h, including Crataegus Fructus extract (A), Pueraria Lobatae Radix extract (B), Atractylodis Macrocephalae Rhizoma extract (C), Salviae Miltiorrhiza Radix et Rhizoma extract (D), Cassiae Semen extract (E), Glycyrrhizae Radix et Rhizoma extract (F), Red Yeast Rice extract (G), Ginkgo Leaves extract (H), Soybean Lecithin (I), and Fish Oil (J). (K) Intracellular lipid droplets in HepG2 cells were stained with Oil Red O and imaged (magnification 40 ×). Control cells (Con) were incubated with 1 % BSA. Prevention group cells (Pre) were treated with 10 tested samples and OA simultaneously for 24 h. Treat group cells (Tre) were treated with OA for 24 h and then supplied with testing samples for an additional 24 h. Values are expressed as mean ± SD. *$p < 0.05$, **$p < 0.01$, ***$p < 0.001$ vs. Con. (For interpretation of the references to colour in this figure legend, the reader is referred to the Web version of this article.)

follows: Crataegus Fructus extract (5 μg/mL), Pueraria Lobatae Radix extract (10 μg/mL), Atractylodis Macrocephalae Rhizoma extract (20 μg/mL), Salviae Miltiorrhiza Radix et Rhizoma extract (20 μg/mL), Cassiae Semen extract (50 μg/mL), Glycyrrhizae Radix et Rhizoma extract (50 μg/mL), Red Yeast Rice extract (20 μg/mL), Ginkgo Leaves extract (100 μg/mL), Soybean Lecithin (100 μg/mL), and Fish Oil (10 μg/mL).

Subsequently, we examined the preventive and therapeutic effects of the tested samples against OA-induced formation and build-up of lipid droplets using Oil Red O staining. The tested samples included extracts from Crataegus Fructus, Pueraria Lobatae Radix, Atractylodis Macrocephalae Rhizoma, Salviae Miltiorrhiza Radix et Rhizoma, Cassiae Semen, Glycyrrhizae Radix et Rhizoma, and Red Yeast Rice. Ginkgo leaves extract, Soybean Lecithin, and Fish Oil were used as controls. The staining results indicated that the Crataegus Fructus extract and Cassiae Semen extract inhibited OA-induced lipid droplets formation, with their preventive effects surpassing their therapeutic effects (Fig. 1K).

Oil Red O staining was employed to determine the optimal ratio of the formula containing KRG, Crataegus Fructus, and Cassiae Semen (Fig. 2A). The optimal proportion was identified as group E, composed of 1.5 g of Red Ginseng extract, 1.8 g of Crataegus Fructus extract and 0.6 g of Cassiae Semen extract, which was abbreviated as KRGF (Korean Red Ginseng Formula).

3.2. KRGF alleviates OA-induced steatosis in HepG2 cells

Before further evaluating the protective effect of KRGF on OA-induced steatosis in HepG2 cells, we assessed cellular viability following treatment with OA and KRGF using the CCK-8 assay. No cytotoxicity was observed in HepG2 cells when the OA concentration was below 1 mM (Fig. 2B). Thus, we chose 0.8 mM as the OA concentration to induce steatosis. KRGF (62.5-2000 μg/mL) exhibited no cytotoxicity on the treated cells, either alone or in combination with 0.8 mM OA (Fig. 2C and D).

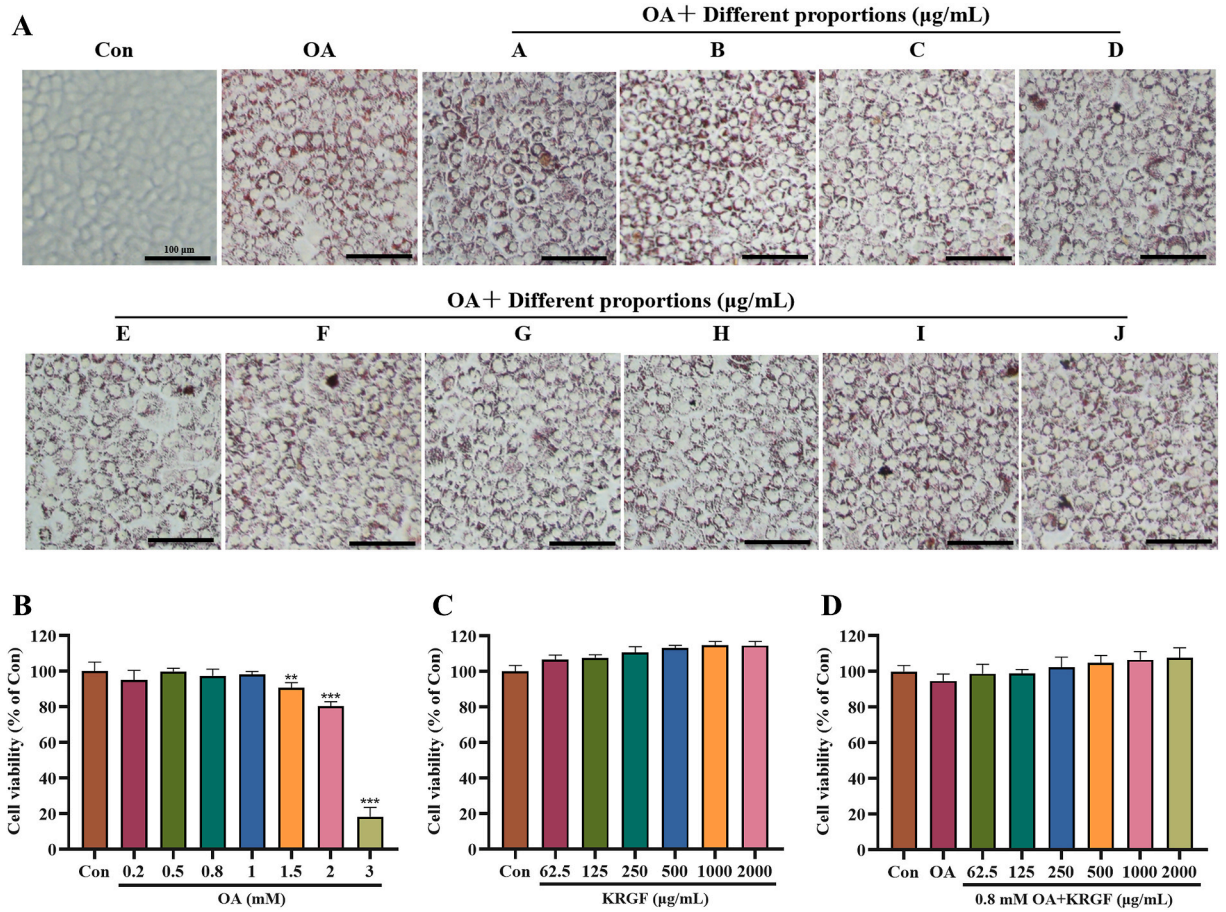

Fig. 2. Effect of different proportions of formula containing Korean Red Ginseng, Crataegus Fructus and Cassiae Semen on OA-induced lipid accumulation in HepG2 cells. (A) Oil Red O staining images of HepG2 cells treated with OA and different proportions of the hypolipidemic formula simultaneously for 24 h. Control cells (Con) were incubated with 1 % BSA. Lipid droplets of HepG2 cells were dyed red (magnification 40 ×). Cell viability was determined after 24 h treatment of different concentrations of OA (B), KRGF (C), and KRGF in the presence of 0.8 mM OA (D), separately. Values are expressed as mean ± SD (n = 2). $^{**}p < 0.01$, $^{***}p < 0.001$ vs. Con. (For interpretation of the references to colour in this figure legend, the reader is referred to the Web version of this article.)

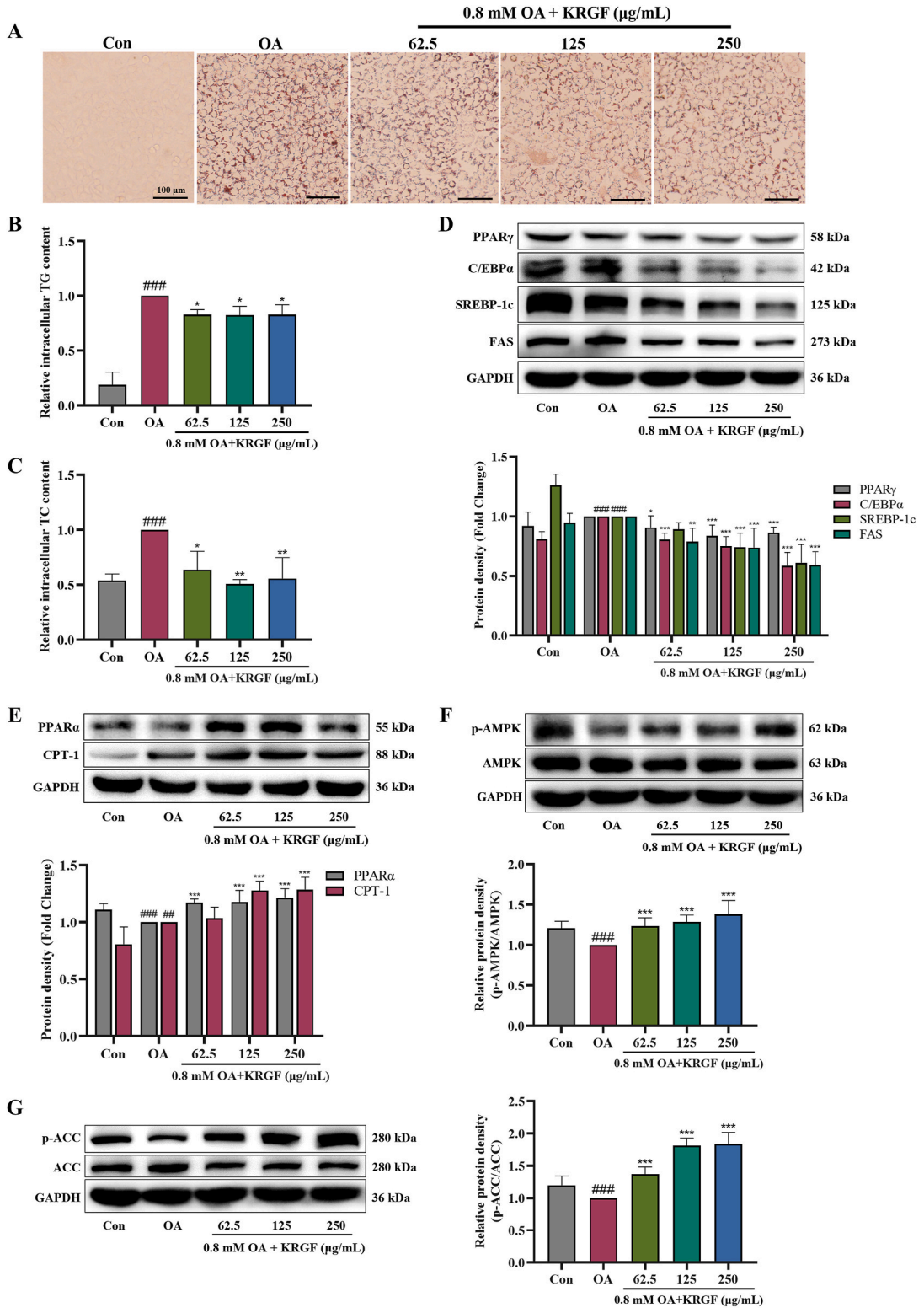

Fig. 3. Effect of Korean Red Ginseng Formula (KRGF) on steatosis HepG2 cells induced by 0.8 mM OA. (A) Images of HepG2 cells stained by Oil Red O after 0.8 mM OA and various concentrations of KRGF application for 24 h. 1 % BSA was utilized for the control cells. At 40 × magnification, red-stained lipid droplets can be observed in the cells. (B) Intracellular triglyceride (TG) quantification. (C) Intracellular total cholesterol (TC) quantification. (D) Western blot results detected the PPARγ, C/EBPα, SREBP-1c, and FAS protein levels in KRGF-treated and OA-treated HepG2 cells. (E) The expression of CPT-1 and PPARα proteins in KRGF-treated and OA-treated HepG2 cells were determined by Western blot. GAPDH confirmed

equal protein loading. Western blot results showed protein levels of (F) *p*-AMPK and (G) *p*-ACC in HepG2 cells treated with KRGF and OA. AMPK and ACC served as loading controls for *p*-AMPK and *p*-ACC. The original images of blots were shown in the Supplementary Material. All experiments were conducted 3 times. HepG2 cells were treated with 0.8 mM OA together with KRGF at 62.5, 125, and 250 μg/mL, and cultured for 24 h. Values are presented as mean ± SD (n = 3). ##p < 0.01, ###p < 0.001 vs. Con; *p < 0.05, **p < 0.01, ***p < 0.001 vs. OA. (For interpretation of the references to colour in this figure legend, the reader is referred to the Web version of this article.)

We selected a concentration range of 62.5-250 μg/mL of KRGF to study its effect on improving cellular steatosis. The effect of KRGF treatment (62.5-250 μg/mL) on lipid droplets formation in HepG2 cells was observed after inducing steatosis using 0.8 mM OA. OA-induced HepG2 cells exhibited numerous red lipid droplets, indicative of steatosis, compared to control cells without OA treatment (Fig. 3A). The decrease in lipid droplets was more pronounced in KRGF-treated cells than in OA-treated cells (Fig. 3A). To confirm the lipid-lowering effect of KRGF, intracellular TG and TC levels were quantitatively measured. KRGF treatment significantly decreased TG and TC levels in the treated cells (Fig. 3B and C). To explore the mechanism of KRGF alleviating steatosis, Western blot analysis revealed that KRGF significantly suppressed the expressions of key regulators in adipogenesis (C/EBPα and PPARγ), as well as lipogenesis-related proteins (SREBP-1c and FAS) in KRGF-treated HepG2 cells compared to OA-induced steatosis HepG2 cells (Fig. 3D). KRGF treatment also significantly upregulated the expression of fatty acid oxidation-related proteins (PPARα and CPT-1) in OA-induced HepG2 cells in a dose-dependent manner (Fig. 3E). Furthermore, a substantial reduction in the expression of *p*-AMPK and *p*-ACC proteins was observed in HepG2 cells after OA induction compared to the control cells. Notably, an increase in AMPK and ACC phosphorylation was observed in KRGF-treated cells compared to that in OA-induced HepG2 cells (Fig. 3F and G).

3.3. KRGF reduces blood lipids and improves hepatic steatosis in HFD-fed rats

Following model establishment, rats were administered with KRGF (325 and 650 mg/kg/day) for 30 days, with fenofibrate serving as a positive control (Fig. 4A). There was no significant difference in initial body weight among all groups (Fig. 4B and C, and Table 2). Compared to the NC group, the HF group showed an 8.6 % increase in final body weight and a 50.3 % increase in the liver index. However, there were no apparent differences in body weight or liver index between the HF and KRGF groups. Despite significantly higher food consumption in the HF group compared to the NC group, the food efficiency ratio (FER) did not differ significantly. The LD group exhibited a considerable decrease in food intake, similar to the PC group, while the HD group's food intake remained unaffected. The FER in the KRGF group did not significantly differ from that in the HF group (Table 2). These results imply that KRGF does not reduce the body weight of NAFLD rats.

We next analyzed changes in serum lipids to investigate the lipid-modifying effects of KRGF treatment in HFD-induced NAFLD rats. HFD significantly elevated serum TG, TC, and LDL-C levels by approximately 1.38-, 1.92-, and 7.8-fold, respectively, compared to the NC group (Fig. 4D–G). The HF group experienced a significant reduction in serum HDL-C, approximately 0.83 times lower than that in the NC group. Following KRGF treatment, serum TG and TC levels significantly decreased, and the effect in the HD group was as good as that in the PC group. However, serum levels of HDL-C and LDL-C were not markedly differed between the HF and KRGF groups (Fig. 4F and G). Collectively, these findings suggest that KRGF exerts a hypolipidemic effect.

H&E staining and measurement of liver lipid content indicated that KRGF improved hepatic steatosis. H&E staining revealed pathological changes in liver tissue. The hepatocytes of the NC rats exhibited normal morphology and orderly arrangement (Fig. 4H). Liver steatosis and fat vacuoles were observed in hepatocytes of the HF group. The KRGF and PC groups demonstrated pronounced improvement in liver steatosis and a reduction in the number of hepatocyte fat vacuoles compared to the HF group. Similar to the PC group, the HD group exhibited a superior ameliorative effect on hepatic steatosis compared to the LD group. The HFD increased liver TG and TC levels in rats by 5.1 and 5.8 times, respectively, compared to those in the NC group (Fig. 4I and J). KRGF supplementation considerably reduced hepatic TG and TC accumulation induced by the HFD, with the TC reduction effect similar to that of the PC group. These findings demonstrate that KRGF alleviates HFD-induced hepatic steatosis.

3.4. KRGF regulates lipogenic regulatory factors in HFD-induced rats

To study the molecular mechanisms underlying KRGF's role in reducing hepatic steatosis, we used qRT-PCR and western blotting to assess the expression of enzymes and regulators associated with lipid synthesis and lipolysis. KRGF supplementation significantly downregulated the mRNA levels of adipogenic transcription factors (PPARγ and C/EBPα) and lipogenic factors (ACC, FAS, and SREBP-1c) compared to the HF group, with inhibitory effects similar to those of the PC group (Fig. 5A–D, Fig. 6C). Consistent with these findings, the levels of SREBP-1c, FAS, PPARγ, and C/EBPα proteins were considerably enhanced in the livers of rats in the HF group compared to those in the NC group. Additionally, the KRGF-supplemented group showed a marked downregulation of SREBP-1c, FAS, PPARγ, and C/EBPα protein levels compared to the HF group (Fig. 5E).

3.5. KRGF increases fatty acid oxidation and activates AMPK and ACC signaling in HFD-induced rats

We investigated the regulation of fatty acid oxidation (FAO) by KRGF through measurement of gene and protein levels of CPT-1 and PPARα. The mRNA levels of PPARα and CPT-1 were significantly upregulated in the KRGF-supplemented groups (Fig. 6A and B). Western blot analysis consistently showed that KRGF treatment increased PPARα and CPT-1 protein levels in a dose-dependent manner compared to those in the HF group (Fig. 6D). Western blot analysis was conducted to assess the effect of KRGF on the activation of

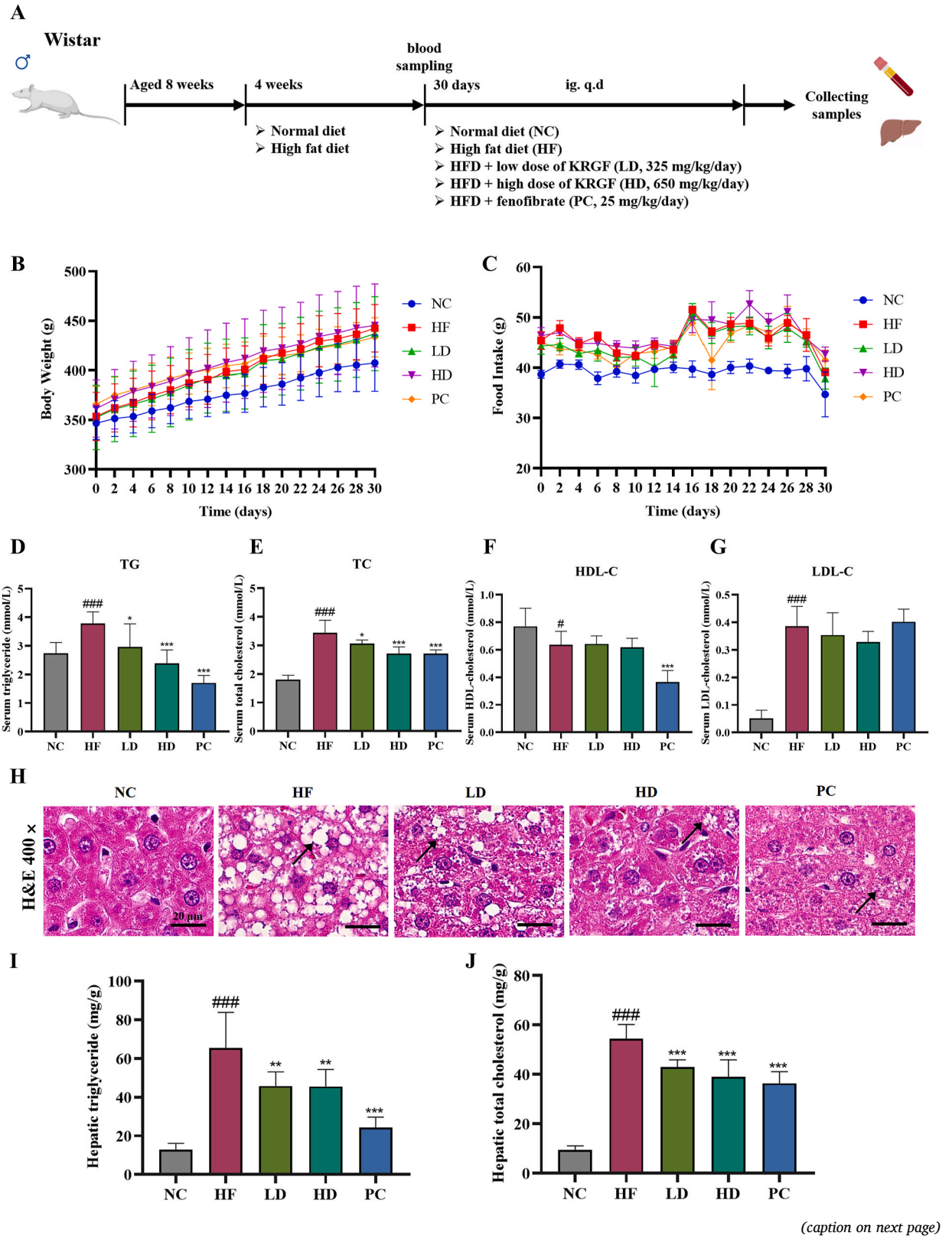

(caption on next page)

Fig. 4. Effect on blood lipids and hepatic steatosis-modifying following 30 days of intragastric administration of KRGF to NAFLD rats induced by high-fat diet (HFD). (A) Flowchart of the experimental procedures. (B–C) The changes in body weight and food intake. (D–G) Levels of serum lipid (TG, TC, HDL-C and LDL-C). (H) Staining of liver tissues with H&E (400 ×). Scale bar = 200 μm. n = 3. Black arrows indicate obvious fatty changes in hepatocytes. (I–J) Hepatic lipid contents (TG and TC). Values are presented as mean ± SD (n = 8). #p < 0.05, ###p < 0.001 vs. NC; *p < 0.05, **p < 0.01, ***p < 0.001 vs. HF.

Table 2
Effects of KRGF on body weight, food intake, food efficacy ratio and liver weight in NAFLD-induced rats (mean ± SD, n = 8).

	NC	HF	LD	HD	PC
Initial BW (g)	346.75 ± 15.83	353.63 ± 23.48	352.63 ± 31.40	361.75 ± 28.06	366.25 ± 17.30
Final BW (g)	407.38 ± 27.32	442.50 ± 23.32#	436.88 ± 36.20	445.25 ± 40.57	433.38 ± 19.05
BW gains (g)	60.63 ± 27.26	88.88 ± 8.32##	84.25 ± 9.43	83.50 ± 17.67	67.13 ± 16.13*
Food intake (g)	588.71 ± 13.96	688.97 ± 5.76###	669.52 ± 22.32*	702.76 ± 7.47	669.54 ± 13.16*
FER (%)	10.25 ± 4.60	12.90 ± 1.19	12.57 ± 1.15	11.89 ± 2.55	10.00 ± 2.29*
Liver weight (g)	11.06 ± 0.87	18.25 ± 1.33###	18.45 ± 1.18	18.65 ± 1.83	18.95 ± 1.48
Liver weight/BW (%)	2.70 ± 0.16	4.06 ± 0.19###	4.10 ± 0.34	4.13 ± 0.22	4.38 ± 0.35

BW, body weight; FER, food efficacy ratio = (body weight gain/food intake) × 100 %; NC, normal control group; HF, HFD-induced control group; LD, HFD + low-dose KRGF (325 mg/kg/day); HD, HFD + high-dose KRGF (650 mg/kg/day); PC, HFD + fenofibrate (25 mg/kg/day). Values are expressed as mean ± SD (n = 8 for each group). #*p* < 0.05, ##*p* < 0.01, ###*p* < 0.001 vs. NC; **p* < 0.05 vs. HF.

AMPK and ACC signaling in HFD-induced rat livers. The decrease in *p*-AMPK and *p*-ACC levels was more pronounced in the HF group than in the NC group. Concurrently, the phosphorylation of AMPK and ACC were activated in a dose-dependent manner in the KRGF-treated group, similar to the PC group (Fig. 6E and F).

3.6. KRGF regulates cholesterol metabolism in HFD-induced rats

To study the molecular mechanisms by which KRGF regulates cholesterol metabolism in NAFLD rats, we assessed the gene expression of key enzymes involved in different metabolic processes in the liver. The key enzymes examined were HMGCR (3-hydroxy-3-methylglutaryl-CoA reductase), which catalyzes cholesterol biosynthesis, ACAT2 (acetyl-CoA acetyltransferase 2), which involves in intestinal cholesterol absorption, apoB (apolipoprotein B), crucial for cholesterol transport, and CYP7A1 (cholesterol 7 alpha-hydroxylase), catalyzing the rate-determining step in the classical anabolic pathway of bile acid [29,30]. The higher levels of HMGCR, ACAT2, and apoB genes in the liver of the HF group compared to the NC group were confirmed by RT-PCR analysis. Similar to the PC group, KRGF administration markedly decreased gene levels (Fig. 7A–C). Moreover, KRGF supplementation increased the mRNA expression of CYP7A1 in a dose-dependent manner compared to that in the HF group (Fig. 7D).

3.7. KRGT manages blood lipids in HFD-fed rats

Considering that the preventive and ameliorative effects of KRGF on NAFLD were complicated by hyperlipidemia, we formulated it into a tablet. We confirmed the blood lipid-regulatory role of KRGT in HFD-fed rats. After establishing the hyperlipidemia model, the rats were treated with KRGT for 30-day at doses of 166.7, 333.3, 666.7, and 1333.3 mg/kg/day (Fig. 8A). The body weight of the HF group increased by 10.2 %, whereas the body weight in the KRGT group was unaffected. Food intake and FER did not differ significantly between the KRGT and HF groups (Fig. 8B and C, and Table 3).

Compared to the NC group, the serum levels of TG, TC, and LDL-C were elevated by 1.84-fold, 2.08-fold, and 3.73-fold, respectively, in the HF group. The HDL-C level in the HF group was 0.83-fold higher than that in the NC group. KRGT notably reduced the TG and TC levels (Fig. 8D and E). However, there was no substantial difference in serum LDL-C and HDL-C levels between the HF and KRGT groups (Fig. 8F and G).

4. Discussion

Triglycerides accumulate in hepatocytes due to excessive calorie intake and obesity, usually resulting in hepatic steatosis and the development of NAFLD [31]. KRG, a traditional medicine extensively used in East Asia, has demonstrated therapeutic effects on insulin resistance, obesity, NAFLD, and other conditions [8,12]. Moreover, Crataegus Fructus and Cassiae Semen are known to lower blood lipid levels and improve NAFLD [13,14]. Using an OA-induced steatosis model in HepG2 cells and a HFD-induced NAFLD rat model, we explored the mechanism of action of KRGF in treating NAFLD. Our findings revealed that the administration of KRGF to OA-induced HepG2 cells decreased TG and TC levels, significantly inhibiting lipid accumulation. This is consistent with a previous study that found that ginseng seed oil suppressed FFA-induced TG accumulation in HepG2 cells [32]. Our experiments with HFD-fed rat further demonstrated fatty liver characteristics, including elevated TG and TC levels, and liver steatosis. Treatment with KRGF and PC significantly diminished liver lipid accumulation and improved HFD-induced hepatic steatosis.

Dysfunction in lipid metabolism leads to substantial triglyceride and cholesterol build-up in hepatocytes, resulting in hepatic steatosis. The main pathological feature of NAFLD is excessive accumulation of triglyceride in the liver due to various factors including

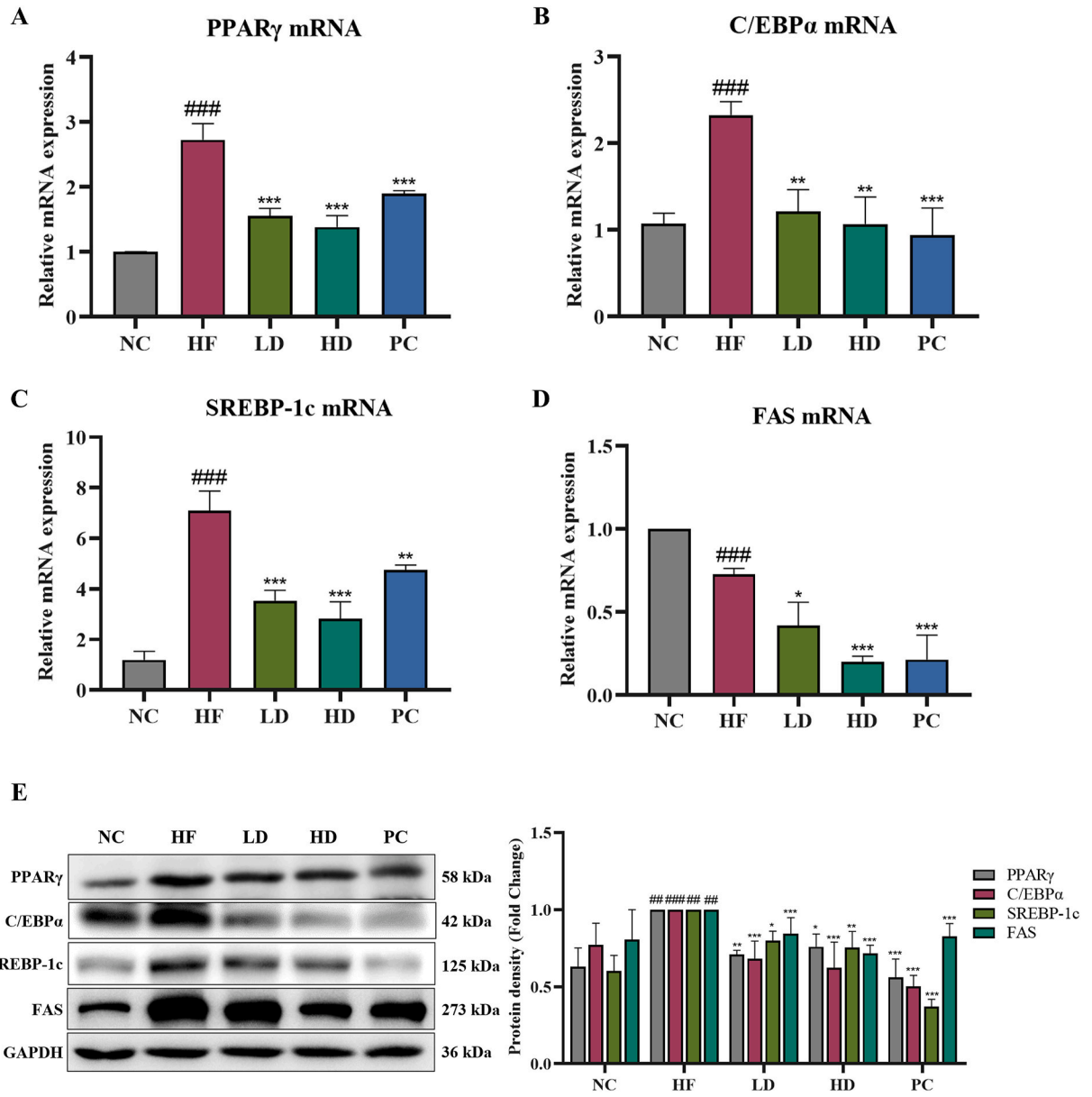

Fig. 5. Effect of KRGF on the level of lipogenic markers in high-fat diet (HFD)-induced rats. Relative PPARγ (A), C/EBPα (B), SREBP-1c (C), and FAS (D) mRNA expressions were standardized to GAPDH. (E) Western blot results indicated the protein expressions of PPARγ, C/EBPα, SREBP-1c, and FAS. The original images of blots were shown in the Supplementary Material. Values are presented as mean ± SD (n = 3). ##p < 0.01 vs. NC, ###p < 0.001; *p < 0.05, **p < 0.01, ***p < 0.001 vs. HF.

increased fatty acid intake, *de novo* lipogenesis (DNL), dysregulated fatty acid oxidation (FAO), and abnormal lipid export. PPARγ and C/EBPα are transcription factors that influence adipogenic differentiation [33–35]. SREBP-1c is crucial for triglyceride synthesis, regulating downstream target genes ACC and FAS, and participating in DNL [36,37]. As an upstream regulator, PPARα promotes fatty acid β-oxidation and decreases fatty acid deposition in the liver by inducing the expression of CPT-1 (the rate-limiting enzyme for FAO) [38]. AMPK regulates enzymes and transcription regulators associated with lipid metabolism, playing a critical role in hepatic lipid homeostasis. Activated AMPK represses fatty acid synthesis and promotes FAO [39].

The role of KRGF in triglyceride metabolism and its molecular regulation were investigated by examining gene and protein expressions related to DNL and FAO. The findings revealed that both KRGF and PC treatment significantly decreased lipogenic factors, such as PPARγ, C/EBPα, SREBP-1c, and FAS. Additionally, KRGF and PC increased the levels of FAO-related regulators, including PPARα and CPT-1, while also elevating AMPK and ACC phosphorylation levels. Overall, our data suggest that KRGF reduces TG accumulation by suppressing lipogenesis and promoting FAO, thereby lowering TG levels and improving hepatic steatosis.

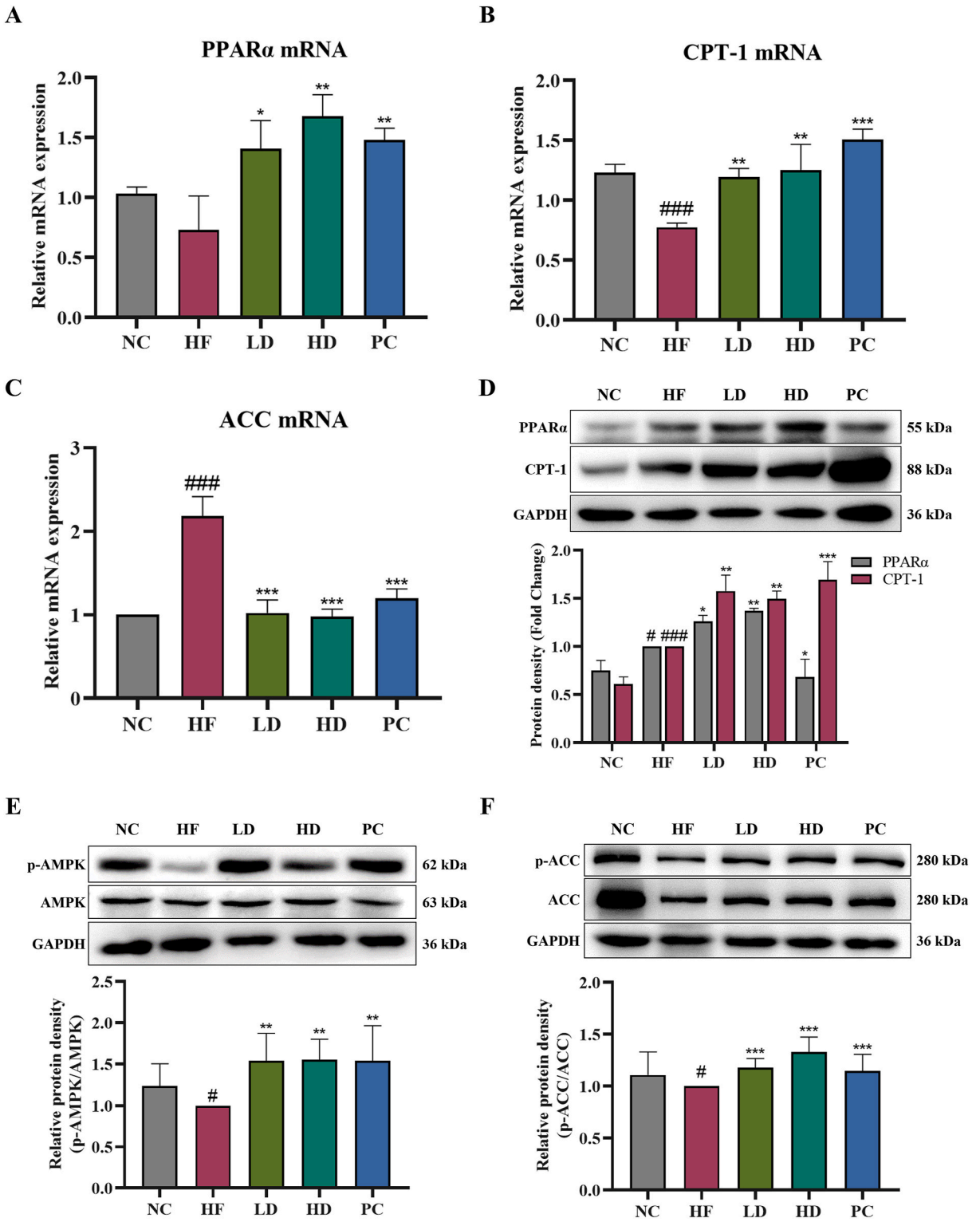

Fig. 6. Effect of KRGF on fatty acid oxidation, and AMPK and ACC signaling in high-fat diet (HFD)-induced rats. (A–C) Relative PPARα (A), CPT-1 (B) and ACC (C) gene expressions were determined by RT-PCR, and GAPDH as an internal reference gene for normalization. (D) Western blot results showing PPARα and CPT-1 protein expression. GAPDH served as an internal reference protein. Western blot detected the phospho-AMPK (*p*-AMPK) (E) and phospho-ACC (*p*-ACC) (F) protein expressions. The original images of blots were shown in the Supplementary Material. Values are presented as mean ± SD (n = 3). #$p < 0.05$, ###$p < 0.001$ vs. NC; *$p < 0.05$, **$p < 0.01$, ***$p < 0.001$ vs. HF.

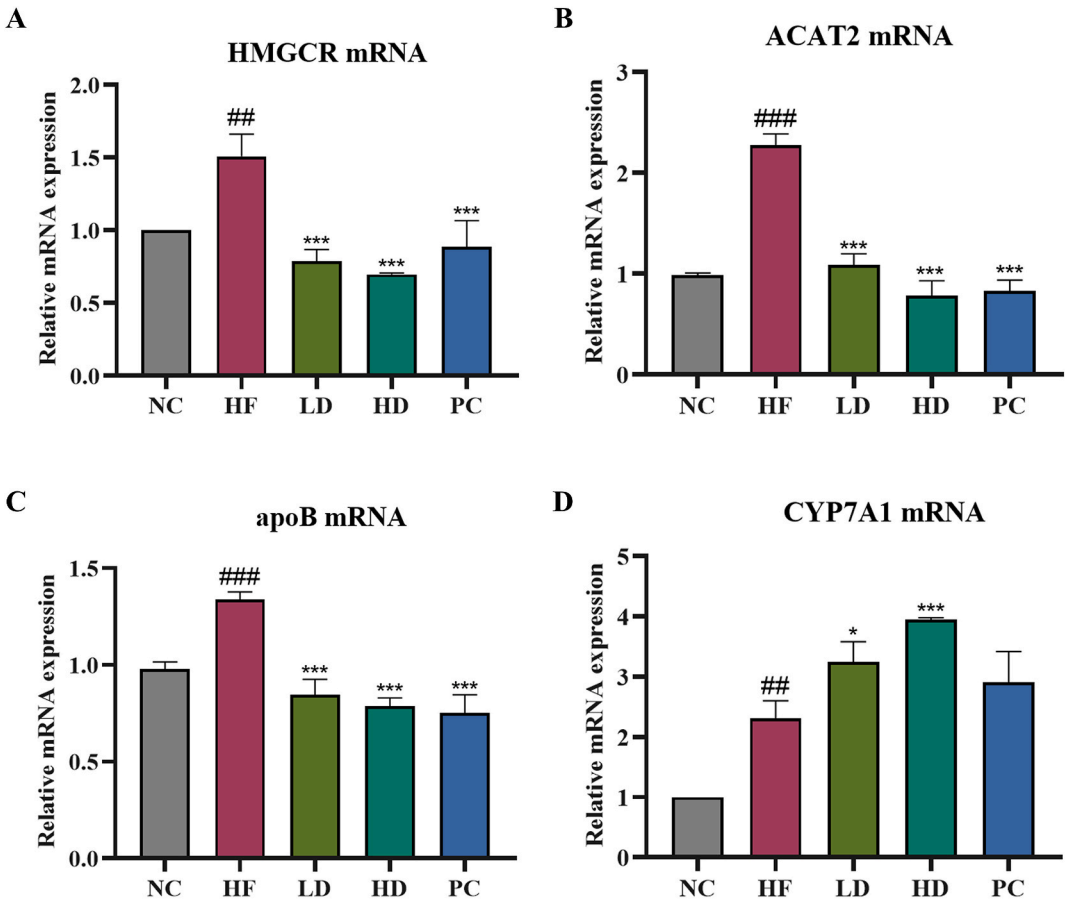

Fig. 7. Effect of KRGF on cholesterol metabolism-related enzymes in high-fat diet (HFD)-induced rats. (A–D) GAPDH gene served as an internal reference for normalizing the expression of HMGCR (A), ACAT2 (B), apoB (C) and CYP7A1 (D) gene. Values are presented as mean ± SD (n = 3). ##p < 0.01, ###p < 0.001 vs. NC; *p < 0.05, ***p < 0.001 vs. HF.

NAFLD is characterized by disrupted hepatic TC homeostasis and altered hepatic TG metabolism. We found that KRGF possesses the remarkable ability to upregulate CYP7A1, a critical enzyme in TC catabolism. Additionally, KRGF downregulates key enzymes in TC accumulation and anabolism, such as ACAT2, HMGCR, and apoB; worth noting PC also exhibits similar effects. These findings indicate that KRGF reduces TC accumulation by suppressing cholesterol synthesis, uptake, and transport, and promoting cholesterol excretion, ultimately lowering TC levels and ameliorating hepatic steatosis.

This study highlights that KRGF mitigates steatosis and decreases blood lipid levels by modulating genes and proteins involved in TC and TG metabolism, thus improving NAFLD complicated by hyperlipidemia.

5. Conclusion

In summary, the present study revealed that KRGF improves OA-induced steatosis and HFD-fed NAFLD by regulating the genes and proteins involved in the metabolism of TC and TG. Furthermore, this study implied that KRGT has the potential to be developed as a supplementary health food for lipid-lowering purpose.

However, this study has several limitations. Firstly, there is a lack of rescue experiments to identify signaling pathway regulated by KRGF, such as by treating HepG2 cells with AMPK inhibitor. To facilitate the advancement of KRGF for clinical use, further mechanistic studies that elucidate its precise molecular pathways are needed, and it is imperative to conduct clinical trials to corroborate its clinical therapeutic value. Additionally, the possible synergistic effects of KRGF when combined with other lipid-lowering agents or lifestyle interventions (such as diet and exercise) are worth exploring to maximize its potential in managing NAFLD and hyperlipidemia.

Ethics statement

The Animal Experiment Ethics Committee of Shanghai University of Traditional Chinese Medicine approved this animal experiment (No. PZSHUTCM201106015; No. PZSHUTCM210709002).

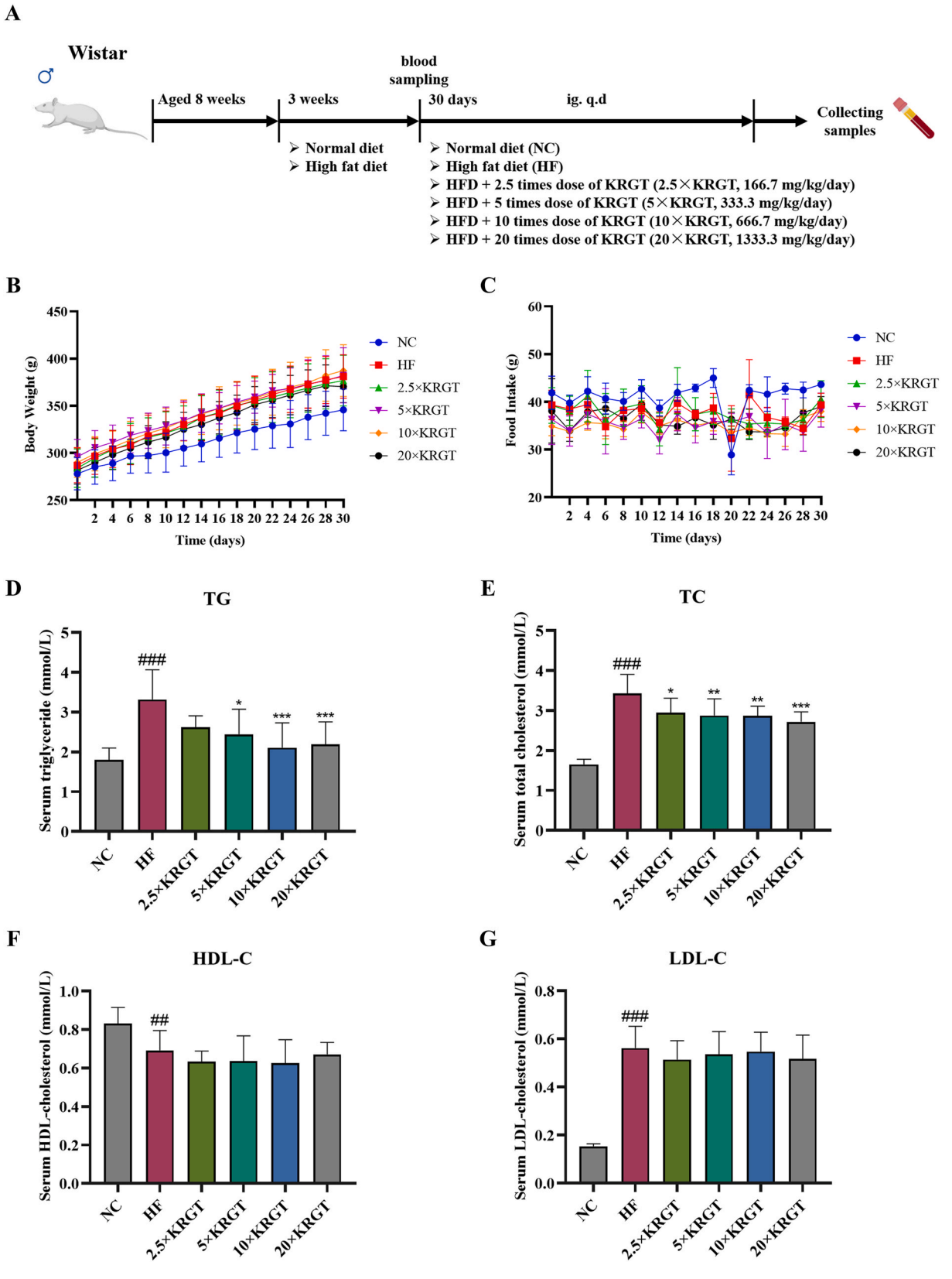

(caption on next page)

Fig. 8. Effect of intragastric administration of KRGT for 30 days on body weight, food intake, and blood lipids in rats induced by high-fat diet (HFD). (A) Flowchart of the experimental procedure. (B–C) Changes in body weight and food intake. (D–G) Serum lipid levels of TG (D), TC (E), HDL-C (F), and LDL-C (G). Values are presented as mean ± SD (n = 9). ##p < 0.01, ###p < 0.001 vs. NC; *p < 0.05, **p < 0.01, ***p < 0.001 vs. HF.

Table 3
Effects of KRGT on body weight, food intake, and food efficacy ratio in NAFLD-induced rats (mean ± SD, n = 9).

	NC	HF	2.5 × KRGT	5 × KRGT	10 × KRGT	20 × KRGT
Initial BW (g)	278.00 ± 16.52	287.00 ± 17.99	283.89 ± 19.74	296.00 ± 17.82	290.11 ± 15.34	281.78 ± 14.31
Final BW (g)	345.78 ± 21.44	381.11 ± 22.25#	376.78 ± 26.01	382.33 ± 28.38	387.33 ± 26.60	370.44 ± 16.51
BW gains (g)	67.78 ± 7.95	94.11 ± 10.17###	92.89 ± 13.84	86.33 ± 23.60	97.22 ± 14.26	88.67 ± 10.19
Food intake (g/day)	615.91 ± 19.48	561.28 ± 18.88###	565.60 ± 44.23	531.68 ± 32.81	528.62 ± 21.04	543.57 ± 10.55
FER (%)	11.00 ± 1.25	16.82 ± 2.21###	16.50 ± 2.71	16.16 ± 4.25	18.35 ± 2.27	16.30 ± 1.73

BW, body weight; FER, food efficacy ratio = (body weight gain/food intake) × 100 %; NC, normal control group; HF, HFD-induced control group; 2.5 × KRGT, HFD + 2.5 times dose of KRGT (166.7 mg/kg/day); 5 × KRGT, HFD + 5 times dose of KRGT (333.3 mg/kg/day); 10 × KRGT, HFD + 10 times dose of KRGT (666.7 mg/kg/day); 20 × KRGT, HFD + 20 times dose of KRGT (1333.3 mg/kg/day). Values are expressed as mean ± SD (n = 9 for each group). #$p < 0.05$, ###$p < 0.001$ vs. NC.

Funding statement

This study was funded by the National Natural Science Foundation of China (No. 82204437), Shanghai Municipality Science and Technology Commission (No. 22YF1445100), Key-Area Research and Development Program of Guangdong Province, China (No. 2020B1111110003), and the Shanghai University of Traditional Chinese Medicine Budget Project: Study on the Anti-gout Mechanism of Fu Tea, a traditional Chinese Fermented Tea (No. 2021LK109).

Data availability statement

Data included in article/supp. material/referenced in article.

CRediT authorship contribution statement

Min Zheng: Conceptualization, Data curation, Formal analysis, Investigation, Validation, Visualization, Writing – original draft, Writing – review & editing. **Yang Li:** Conceptualization, Data curation, Formal analysis, Investigation, Validation, Visualization, Writing – original draft, Writing – review & editing. **Zhiying Dong:** Formal analysis, Visualization, Writing – original draft, Writing – review & editing. **Yibo Zhang:** Formal analysis, Visualization, Writing – original draft, Writing – review & editing. **Zhichao Xi:** Conceptualization, Writing – review & editing. **Man Yuan:** Funding acquisition, Resources, Software, Writing – review & editing. **Hongxi Xu:** Conceptualization, Funding acquisition, Project administration, Resources, Software, Supervision.

Declaration of competing interest

The authors declare the following financial interests/personal relationships which may be considered as potential competing interests:Hongxi Xu has patent pending to 202211165335.X.

Appendix A. Supplementary data

Supplementary data to this article can be found online at https://doi.org/10.1016/j.heliyon.2023.e21846.

References

[1] Z. Younossi, F. Tacke, M. Arrese, B. Chander Sharma, I. Mostafa, E. Bugianesi, V. Wai-Sun Wong, Y. Yilmaz, J. George, J. Fan, M.B. Vos, Global perspectives on nonalcoholic fatty liver disease and nonalcoholic steatohepatitis, Hepatology 69 (6) (2019) 2672–2682.
[2] F. Zhou, J. Zhou, W. Wang, X.J. Zhang, Y.X. Ji, P. Zhang, Z.G. She, L. Zhu, J. Cai, H. Li, Unexpected rapid increase in the burden of NAFLD in China from 2008 to 2018: a systematic review and meta-analysis, Hepatology 70 (4) (2019) 1119–1133.
[3] K. Riazi, H. Azhari, J.H. Charette, F.E. Underwood, J.A. King, E.E. Afshar, M.G. Swain, S.E. Congly, G.G. Kaplan, A.A. Shaheen, The prevalence and incidence of NAFLD worldwide: a systematic review and meta-analysis, Lancet Gastroenterol Hepatol 7 (9) (2022) 851–861.
[4] A.J. Sanyal, E.M. Brunt, D.E. Kleiner, K.V. Kowdley, N. Chalasani, J.E. Lavine, V. Ratziu, A. McCullough, Endpoints and clinical trial design for nonalcoholic steatohepatitis, Hepatology 54 (1) (2011) 344–353.
[5] H. Tilg, A.R. Moschen, Evolution of inflammation in nonalcoholic fatty liver disease: the multiple parallel hits hypothesis, Hepatology 52 (5) (2010) 1836–1846.
[6] E. Buzzetti, M. Pinzani, E.A. Tsochatzis, The multiple-hit pathogenesis of non-alcoholic fatty liver disease (NAFLD), Metabolism 65 (8) (2016) 1038–1048.

[7] S.L. Friedman, B.A. Neuschwander-Tetri, M. Rinella, A.J. Sanyal, Mechanisms of NAFLD development and therapeutic strategies, Nat Med 24 (7) (2018) 908–922.

[8] S.J. Yoon, S.K. Kim, N.Y. Lee, Y.R. Choi, H.S. Kim, H. Gupta, G.S. Youn, H. Sung, M.J. Shin, K.T. Suk, Effect of Korean red ginseng on metabolic syndrome, J Ginseng Res 45 (3) (2021) 380–389.

[9] S.H. Hong, K.T. Suk, S.H. Choi, J.W. Lee, H.T. Sung, C.H. Kim, E.J. Kim, M.J. Kim, S.H. Han, M.Y. Kim, S.K. Baik, D.J. Kim, G.J. Lee, S.K. Lee, S.H. Park, O. H. Ryu, Anti-oxidant and natural killer cell activity of Korean red ginseng (*Panax ginseng*) and urushiol (*Rhus vernicifera* Stokes) on non-alcoholic fatty liver disease of rat, Food Chem. Toxicol. 55 (2013) 586–591.

[10] S.Y. Choi, J.S. Park, C.H. Shon, C.Y. Lee, J.M. Ryu, D.J. Son, B.Y. Hwang, H.S. Yoo, Y.C. Cho, J. Lee, J.W. Kim, Y.S. Roh, Fermented Korean red ginseng extract enriched in rd and Rg3 protects against non-alcoholic fatty liver disease through regulation of mTORC1, Nutrients 11 (12) (2019).

[11] Y. Zheng, J. Lee, E.H. Lee, G. In, J. Kim, M.H. Lee, O.H. Lee, I.J. Kang, A combination of Korean red ginseng extract and Glycyrrhiza glabra L. Extract enhances their individual anti-obesity properties in 3T3-L1 adipocytes and C57bl/6J obese mice, J. Med. Food 23 (3) (2020) 215–223.

[12] Q. Zhang, L. Zhang, K. Liu, H. Shang, J. Ruan, Z. Yu, S. Meng, F. Liang, T. Wang, H. Zhang, W. Peng, Y. Wang, J. Chen, T. Xiao, B. Wang, A network pharmacology study on the active components and targets of the radix ginseng and radix Bupleuri herb pair for treating nonalcoholic fatty liver disease, Evid Based Complement Alternat Med 2022 (2022), 1638740.

[13] G. Saeedi, F. Jeivad, M. Goharbari, G.H. Gheshlaghi, O. Sabzevari, Ethanol extract of Crataegus oxyacantha L. Ameliorate dietary non-alcoholic fatty liver disease in rat, Drug Res. 68 (10) (2018) 553–559.

[14] H. Luo, H. Wu, L. Wang, S. Xiao, Y. Lu, C. Liu, X. Yu, X. Zhang, Z. Wang, L. Tang, Hepatoprotective effects of Cassiae Semen on mice with non-alcoholic fatty liver disease based on gut microbiota, Commun. Biol. 4 (1) (2021) 1357.

[15] J.J. Lee, H.J. Lee, S.W. Oh, Antiobesity effects of sansa (crataegi fructus) on 3T3-L1 cells and on high-fat-high-cholesterol diet-induced obese rats, J. Med. Food 20 (1) (2017) 19–29.

[16] F. Zhou, M. Ding, Y. Gu, G. Fan, C. Liu, Y. Li, R. Sun, J. Wu, J. Li, X. Xue, H. Li, X. Li, Aurantio-obtusin attenuates non-alcoholic fatty liver disease through AMPK-mediated autophagy and fatty acid oxidation pathways, Front. Pharmacol. 12 (2021), 826628.

[17] J. Yang, A. Zhu, S. Xiao, T. Zhang, L. Wang, Q. Wang, L. Han, Anthraquinones in the aqueous extract of Cassiae semen cause liver injury in rats through lipid metabolism disorder, Phytomedicine 64 (2019), 153059.

[18] D.W. Lim, M. Song, J. Park, S.W. Park, N.H. Kim, B.P. Gaire, H.Y. Choi, H. Kim, Anti-obesity effect of HT048, a herbal combination, in high fat diet-induced obese rats, Molecules 17 (12) (2012) 14765–14777.

[19] J.W. Yun, Possible anti-obesity therapeutics from nature–a review, Phytochemistry 71 (14–15) (2010) 1625–1641.

[20] Y.S. Liu, M.H. Yuan, C.Y. Zhang, H.M. Liu, J.R. Liu, A.L. Wei, Q. Ye, B. Zeng, M.F. Li, Y.P. Guo, L. Guo, Puerariae Lobatae radix flavonoids and puerarin alleviate alcoholic liver injury in zebrafish by regulating alcohol and lipid metabolism, Biomed. Pharmacother. 134 (2021), 111121.

[21] J.H. Wang, S. Bose, H.G. Kim, K.S. Han, H. Kim, Fermented Rhizoma Atractylodis Macrocephalae alleviates high fat diet-induced obesity in association with regulation of intestinal permeability and microbiota in rats, Sci. Rep. 5 (2015) 8391.

[22] Ling-Ling, Clinical application of gaofang(medicated Paste)in cardiovascular disease, H N A Q-Q Z A M-H M A Y-J Z A T-J W A J L A D-Y F A, Chinese Medcine and Culture 5 (3) (2022).

[23] C.J. Liou, Y.K. Lee, N.C. Ting, Y.L. Chen, S.C. Shen, S.J. Wu, W.C. Huang, Protective effects of licochalcone A ameliorates obesity and non-alcoholic fatty liver disease via promotion of the sirt-1/AMPK pathway in mice fed a high-fat diet, Cells 8 (5) (2019).

[24] A.F.G. Cicero, F. Fogacci, M. Banach, Red Yeast Rice for hypercholesterolemia, Methodist Debakey Cardiovasc J 15 (3) (2019) 192–199.

[25] X. Chen, L. Li, X. Liu, R. Luo, G. Liao, L. Li, J. Liu, J. Cheng, Y. Lu, Y. Chen, Oleic acid protects saturated fatty acid mediated lipotoxicity in hepatocytes and rat of non-alcoholic steatohepatitis, Life Sci. 203 (2018) 291–304.

[26] M. Izdebska, I. Piątkowska-Chmiel, A. Korolczuk, M. Herbet, M. Gawrońska-Grzywacz, R. Gieroba, M. Sysa, K. Czajkowska-Bania, M. Cygal, A. Korga, J. Dudka, The beneficial effects of resveratrol on steatosis and mitochondrial oxidative stress in HepG2 cells, Can. J. Physiol. Pharmacol. 95 (12) (2017) 1442–1453.

[27] M. Park, J.H. Yoo, Y.S. Lee, E.J. Park, H.J. Lee, Ameliorative effects of black ginseng on nonalcoholic fatty liver disease in free fatty acid-induced HepG2 cells and high-fat/high-fructose diet-fed mice, J Ginseng Res 44 (2) (2020) 350–361.

[28] X. Jiang, Y. Li, J.L. Feng, W.N. Nik Nabil, R. Wu, Y. Lu, H. Liu, Z.C. Xi, H.X. Xu, Safrana l prevents prostate cancer recurrence by blocking the Re-activation of quiescent cancer cells via downregulation of S-phase kinase-associated protein 2, Front. Cell Dev. Biol. 8 (2020), 598620.

[29] J. Luo, H. Yang, B.L. Song, Mechanisms and regulation of cholesterol homeostasis, Nat. Rev. Mol. Cell Biol. 21 (4) (2020) 225–245.

[30] X. Li, Y. Zu, G. Li, D. Xiang, C. Zhang, D. Liu, Molecular mechanisms of transporter regulation and their impairment in intrahepatic cholestasis, Acta Materia Medica 1 (3) (2022) 381–391.

[31] M. Alves-Bezerra, D.E. Cohen, Triglyceride metabolism in the liver, Compr. Physiol. 8 (1) (2017) 1–8.

[32] G.W. Kim, H.K. Jo, S.H. Chung, Ginseng seed oil ameliorates hepatic lipid accumulation *in vitro* and *in vivo*, J Ginseng Res 42 (4) (2018) 419–428.

[33] A. Guru, P.K. Issac, M. Velayutham, N.T. Saraswathi, A. Arshad, J. Arockiaraj, Molecular mechanism of down-regulating adipogenic transcription factors in 3T3-L1 adipocyte cells by bioactive anti-adipogenic compounds, Mol. Biol. Rep. 48 (1) (2021) 743–761.

[34] P. Tontonoz, E. Hu, B.M. Spiegelman, Stimulation of adipogenesis in fibroblasts by PPAR gamma 2, a lipid-activated transcription factor, Cell 79 (7) (1994) 1147–1156.

[35] L.L. Listenberger, X. Han, S.E. Lewis, S. Cases, R.V. Farese Jr., D.S. Ory, J.E. Schaffer, Triglyceride accumulation protects against fatty acid-induced lipotoxicity, Proc Natl Acad Sci U S A 100 (6) (2003) 3077–3082.

[36] X. Li, Y. Li, W. Yang, C. Xiao, S. Fu, Q. Deng, H. Ding, Z. Wang, G. Liu, X. Li, SREBP-1c overexpression induces triglycerides accumulation through increasing lipid synthesis and decreasing lipid oxidation and VLDL assembly in bovine hepatocytes, J. Steroid Biochem. Mol. Biol. 143 (2014) 174–182.

[37] N. Higuchi, M. Kato, Y. Shundo, H. Tajiri, M. Tanaka, N. Yamashita, M. Kohjima, K. Kotoh, M. Nakamuta, R. Takayanagi, M. Enjoji, Liver X receptor in cooperation with SREBP-1c is a major lipid synthesis regulator in nonalcoholic fatty liver disease, Hepatol. Res. 38 (11) (2008) 1122–1129.

[38] G. Musso, R. Gambino, M. Cassader, Recent insights into hepatic lipid metabolism in non-alcoholic fatty liver disease (NAFLD), Prog. Lipid Res. 48 (1) (2009) 1–26.

[39] Y.H. Li, J. Luo, Y.Y. Mosley, V.E. Hedrick, L.N. Paul, J. Chang, G. Zhang, Y.K. Wang, M.R. Banko, A. Brunet, S. Kuang, J.L. Wu, C.J. Chang, M.P. Scott, J.Y. Yang, AMP-activated protein kinase directly phosphorylates and destabilizes hedgehog pathway transcription factor GLI1 in medulloblastoma, Cell Rep. 12 (4) (2015) 599–609.